Increasing the robustness of electrodynamic WPT systems with hybrid electromechanical transduction

Adrien Ameye, Nicolas Decroix, David Gibus, Nicolas Garraud, Pierre Gasnier, Adrien Badel

Increasing the robustness of electrodynamic WPT systems with hybrid electromechanical transduction

Adrien AMEYE[1,2], Nicolas DECROIX[1,2], David GIBUS[2], Nicolas GARRAUD[1], Pierre GASNIER[1], Adrien BADEL[2]
[1]*Univ. Grenoble Alpes, CEA, Leti, F-38000 Grenoble, France*
[2]*SYMME, Université Savoie Mont-Blanc, Annecy, France*
Email: nicolas.garraud@cea.fr

Received xxxxxxx
Accepted for publication xxxxxx
Published xxxxxx

Abstract

In this paper, we compare the electrical damping capability of low-frequency electrodynamic wireless power transmission (EWPT) systems based on a resonant electromechanical receiver in the context of increasing their mechanical robustness. This study is carried out for piezoelectric (PE) and electrodynamic (ED) transducers. The receiver studied, excited by a distant transmitter coil, consists of a magnet and a resonant cantilever beam, and both ED and PE transducers (hybrid system). A strategy based on dual energy conversion is proposed that takes advantage of each transduction characteristic: the receiver with high-quality-factor is sufficiently sensitive to very weak excitation fields far from the transmitter, while it is robust to strong magnetic fields close to the transmitter by damping its motion. This approach is particularly relevant to increase the robustness of resonant receivers powering moving sensor nodes as the field strength seen by the receiver can vary greatly.
This paper aims to evaluate three energy transduction strategies (PE-only, ED-only and hybrid) to both harvest more power and increase EWPT systems robustness by overdamping. An analytical model of the system is presented along with comparison with experimental results from a 71.7 cm^3 prototype. When the motion amplitude is limited to 0.7 mm to limit aging, the receiver output 19 mW which outperforms the PE and ED modes alone by a factor of 1.5 and 1.8, respectively. Furthermore, the hybrid receiver can limit the amplitude of motion to 0.7 mm under a magnetic field up to 3.6 mT, which is 2.5 and 1.2 times higher than PE and ED alone, respectively.

Keywords: Wireless power transfer, electrodynamic WPT, hybrid transduction, piezoelectric transducer, electrodynamic transducer, low frequency WPT.

Nomenclature

Transmitter-receiver interaction			
d	Transmitter-receiver distance		[m]
B_0	Magnetic field induction amplitude at the receiver location		[T]
F_{eq}	Interaction force acting on the receiver magnet		[N]
m	Magnetic moment	4.46	[A.m^2]
Mechanical system			
M	Equivalent mass	35.3	[g]
L	Equivalent length of the beam	45.0	[mm]
D	Mechanical damping	0.418*	[N.s/m]
Q	Mechanical quality factor	26*	[1]
K	Mechanical stiffness	3350*	[N.m^{-1}]
X	Motion amplitude of the center of the magnets		[m]
X_l	Max. amplitude limitation	0.7	[mm]
Piezoelectric (PE) transducer			
α_{PE}	Piezoelectric coefficient	9.79	[mN/V]
C_p	Parasitic capacitance	421	[nF]
Γ_{PE}	Piezoelectric coupling	0.88*	[1]
$R_{l,PE}$	Resistive load on PE		[Ω]
Electrodynamic (ED) transducer			
β_{ED}	Electrodynamic coefficient	14.4	[N/A]
R_c	Series resistance	121	[Ω]
Γ_{ED}	Electrodynamic coupling	4.10*	[1]
$R_{l,ED}$	Resistive load on ED		[Ω]

*Values determined for X = 0.7 mm

1 Introduction

Whether a wireless sensor node (WSN) operates in a harsh environment subjected to high pressure or temperature, or when it is inaccessible, isolated behind a conductive media, it may be difficult to power it with batteries or through wires. One solution is to harvest ambient energy such as mechanical vibrational energy, light or air flows [1]. When these energy sources are not available, adequate or sufficient, it can be necessary to use a wireless power transmission (WPT) system.

These last ten years, WPT is a growing area in the research community. A multitude of wireless power transmission technologies exist. They are mostly based on magnetic induction principle, far field radio frequency [2], capacitive coupling [3], or acoustic coupling [4]. Previous solutions based on electromagnetic waves operate at high frequencies, which makes it difficult to pass through conductive media such as metal walls or salt water. In addition, limiting electromagnetic interferences in open space can be challenging.

Electrodynamic wireless power transmission (EWPT) is an emerging technology operating at very low frequency that overcomes some of these limitations. It consists of a transmitter, typically a coil, generating a low-frequency magnetic field, and a power receiver comprising a magnet attached to a mechanical system. The mechanical energy of the moving magnet is converted back into electrical energy thanks to an electromechanical transducer (Figure 1).

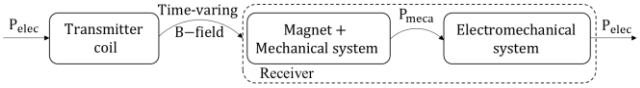

Figure 1: Operating principle of EWPT systems, converting time-varying magnetic fields generated by the transmitter into mechanical power and electrical power.

This technology allows the input power to be transferred through very low frequency alternating magnetic fields (<1 kHz), and therefore to pass safely through conductive media such as thin metal plates, salt water or human body [5].

The literature distinguishes two different topologies of EWPT systems depending on the type of mechanical motion and the electromechanical transduction system used. The first topology includes systems based on a continuously rotating magnet in the receiver [6],[7]. In this case, the magnetic field drives in continuous rotation the permanent magnet placed near or inside a receiver coil harvesting power. This receiver topology presents a high power density, but suffers from a complex control to both start the system and avoid pull-out at high frequencies [8]. The second topology includes systems based on a magnet attached to a resonant mechanical system. The magnetic field excites the system at its resonance frequency. In this case, piezoelectric (PE) [9], electrodynamic (ED) [10], or electrostatic [11] transductions are usually used to convert mechanical energy into electrical energy. This receiver topology presents a lower power density, but has the advantage, thanks to their high-quality factor, of being receptive to low magnetic field amplitude and therefore being able to operate over a larger distance. This work focuses on improving the performances of resonant systems for EWPT.

One of the main challenges facing resonant systems is their poor robustness and ageing, especially when submitted to high motion amplitude. This occurs when the transmitter emits high magnetic fields or when the receiver is close to the transmitter. A simple solution is to use mechanical stoppers [12], [13]. However, repeated shocks lead to overstress, which could also affect the durability of mechanical systems. For this reason, the approach studied in this article to protect the structure in the event of high field inputs is to damp the amplitude of the receiver movement by electrical means, while harvesting energy through PE and ED transducers. In this article, we propose to reduce the maximum displacement amplitude of the receiver during the most important excitation phases, consequently increasing its robustness and lifetime. To achieve this, we choose to combine PE and ED transducers to electrically overdamp the system while still harvesting energy.

Each transduction means have their specific characteristics. PE transducers provide high output voltages and have low internal losses. However, PE transducers are fragile and have limited coupling, unless using high performance piezoelectric materials such as single crystals which are very expensive. On the other hand, ED transducers are less expensive but have intrinsic resistive losses and are less compact than PE systems at equivalent coupling.

The operating principle of vibrational EWPT is analogous to vibrational energy harvesting systems. In this domain, numerous hybrid solutions with multiple transducers have already been investigated, mostly to increase the total power output of the system for a given input acceleration. Jung et al. [14] has shown the interest of multiplying weakly coupled transducers in order to increase the overall output power. Toyabur et al. [15] also introduced a PE-ED hybrid device with multiple resonance frequencies to recover energy at different frequencies. Finally, Wang et al. [16] proposed a tri-hybrid multi-stable prototype including triboelectric transducers in addition of PE and ED transducers reaching a high normalized power density. These studies mainly focused on increasing the electromechanical coupling to increase the power density. None of them highlighted the interest of hybridization from a robustness standpoint.

Concerning the WPT domain, recent works have been done on hybrid systems. In 2022, Halim et al. [17] proposed an analytical model and an experimental validation with a PE-ED hybrid receiver. The new design enables a high power density in a chip-sized device of 0.09 cm^3. In 2022, Truong et al. [18] showed that there is a coupling limit above which hybrid systems are not interesting for increasing the power output. These works on hybrid WPT systems have only focused on increasing the output power and power density of the receiver.

While the robustness of vibrating systems is a prerequisite for their widespread adoption, the limitation of mechanical amplitude during operation by electrical overdamping has not been addressed in the literature for wireless power transmission. In the field of vibrational energy harvesting, [19] in particular has outlined the maximum energy production under constrained amplitude, addressing overdamping in an energy harvester equipped

with a velocity-damping transducer (case of an ED transducer without losses) and equipped with a Coulomb-force transducer (case of a PE transducer without electrical stiffness). [20] has proposed the expression of the maximum recoverable power by a vibrating system under constrained amplitude through a non-linear load in the case of Coulomb-force and velocity-damping transducers.

Complementarily, in this paper, we aim to evaluate the amplitude-limiting capability of real electrodynamic and piezoelectric transducers, whether used individually or in combination (hybrid system). We take into account the electrical losses in the electromagnetic transducer, as well as the change in stiffness due to the electrical charge in the case of the piezoelectric transducer.

This paper aims to assess whether a hybrid transduction can increase the robustness of EWPT resonant systems. The emphasis of this study is not on the overall optimization of the prototype.

The next section introduces the EWPT principle and the materials and method. The third section details the analytical model of the receiver and the identification of the different parameters needed for the simulations in section 4. Finally, the model is validated experimentally, and we discuss about the advantages of hybrid vibrational systems over single transduction ones.

2 Materials and method

2.1 Operating principle of hybrid EWPT

The operating principle of the proposed hybrid system is shown in Figure 2. The transmitter is a coil supplied by an AC current creating a variable magnetic field in its surrounding. The receiver, placed at a distance d from the transmitter coil, is based on a cantilever beam with a permanent magnet attached on its tip. The time-varying magnetic field interacts with the permanent magnet and generates a varying torque on the beam. Two electromechanical transducers are used to convert mechanical energy into electrical energy. Receiver coils placed around the magnet (ED transduction) and piezoelectric patches attached on the beam (PE transduction) are connected to two independent resistive loads to convert energy.

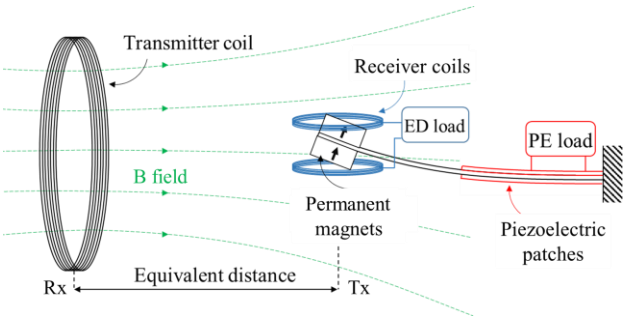

Figure 2: Schematic of the EWPT solution with a hybrid receiver near a transmitter coil (not to scale).

2.2 Proposed method

In this paper, we propose to compare experimental results with theoretical results (Figure 3). The first phase of the study consists of developing a theoretical model presented in section 3. This model is fed by the physical parameters of the hybrid prototype identified by impedance analysis as shown in section 4. The second phase consists of experimentally measuring the output powers of the device as a function of the amplitude and the frequency of the magnetic field as shown in section 5. Finally, the experimental and theoretical performances are compared and discussed.

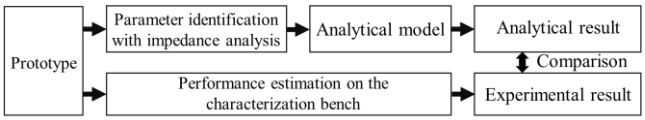

Figure 3: Method applied in this work.

2.3 Proposed prototype

A hybrid receiver prototype shown in Figure 4 was built. It consists of a permanent magnet attached to the end of a piezoelectric beam whose base is clamped. The beam used is a commercially available cantilever (MIDE S452-J1FR-1808XB) with a length of 54 mm, a width of 25.4 mm, and a thickness of 1.32 mm. The four 0.15-mm-thick 956-mm^2 piezoelectric patches are positioned at 70 µm and 250 µm of the neutral axis. Two cylindrical permanent magnets (diameter of 25 mm, height of 5 mm) with a total magnetic moment m of 4.46 A.m^2 are glued at the end of the beam. The equivalent length of the beam L is 45 mm. The two coils at the receiver side have an inner diameter of 29 mm, an outer diameter of 33 mm, and a height of 9 mm. The volume of the smallest rectangular cuboid enclosing the receiver is 35×64×32 mm^3 (71.7 cm^3).

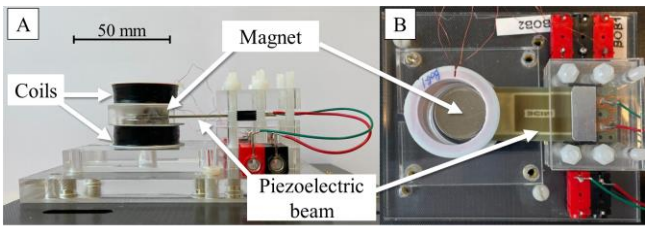

Figure 4: (A) Side view and (B) top view of the proposed hybrid receiver.

2.4 Characterization bench

The test bench used to characterize the performances of the receiver as a function of the magnetic field amplitude B_0 is shown in Figure 5. The receiver is placed at the center of Helmholtz coils (used as transmitter) to allow a fine control of the magnetic field generated at the receiver location. The Helmholtz coils used are from 3B Scientific and have a diameter of 300 mm, a thickness of 24 mm, a width of 26 mm, and are spaced by 150 mm. A multipurpose acquisition system (USB-6366, National Instruments) and a power amplifier (AE Techron 7224) are used to drive the Helmholtz coils with an AC current at constant amplitude. The terminals of each transducer are connected to two programmable resistors, and the voltage across them is monitored by the acquisition system. Finally, a laser

vibrometer (Polytec IVS-500) measures the magnet's motion amplitude.

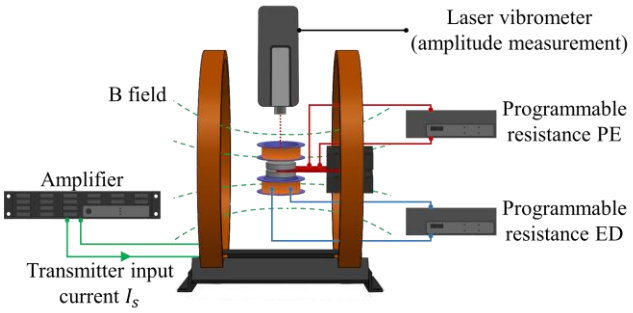

Figure 5: Test bench for performances characterization: the hybrid receiver is placed at the center of Helmholtz coils.

In this experimental setup, the magnets are subjected to a magnetic torque τ defined by:

$$\tau = mB_0 \cos(\omega_e t) \quad (1)$$

Around the first bending mode of resonance, it can be shown that this torque is equivalent to an equivalent force F_{eq} applied at the center of the magnets:

$$F_{eq} = \frac{3\,\tau}{2\,L} \quad (2)$$

The distance between the transmitter and the receiver is emulated by varying the magnetic field at the center of the Helmholtz coils. Figure 6 shows the evolution of the magnetic field amplitude B_0 and the equivalent force F_{eq} with the distance between the receiver and a single coil from the Helmholtz coils for 50 W input power. The equivalent force generated by the transmitter on the receiver magnets is maximum at the center of the coil and decreases rapidly to the power of three with the distance d far from the coil. The force generated by the magnetic gradient from the transmitter on the magnets is small and negligible, especially in the configuration shown in Figure 2.

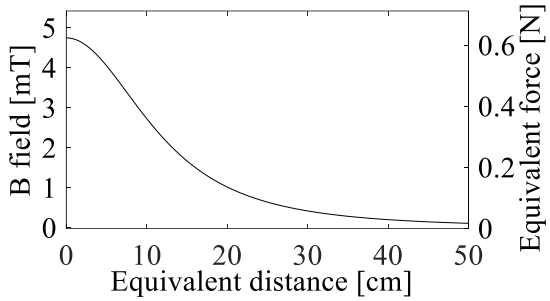

Figure 6: Magnetic field amplitude B_0 and equivalent excitation force F_{eq} at the center of the magnets as a function of the distance d.

With this setup, for given resistive loads, given magnetic field frequency and amplitude B_0, measurements consist of recording the motion amplitude and the output powers generated by the two transducers on the two resistive loads.

3 Theoretical model

This section details an analytical model of a hybrid system. Since the electromechanical transducers are connected to independent resistive loads, the interaction between the two transducers only occurs through the mechanical system. Therefore, the models of the two transducers are first treated independently.

3.1 Mechanical model of the receiver

The receiver is modelled as a mass-spring-damper system excited by the force F_{eq} generated by the interaction of the magnetic field B_0 and the permanent magnets (Figure 7). The mass, the mechanical stiffness, and the mechanical damping are named M, K and D, respectively. The two electromechanical transducers are modelled as stiffeners and dampers. The electrical energy dissipated in the transducers' dampers corresponds to the electrical energy extracted, including the usable energy and the electrical losses. K_{PE} and K_{ED} are the electrical stiffnesses induced by the PE and ED transducers respectively. D_{PE} and D_{ED} are the electrical dampings of the PE and ED transducers respectively, and $D_e = D_{PE} + D_{ED}$ is the total electrical damping.

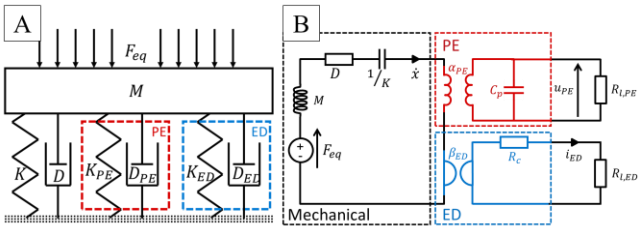

Figure 7: (A) Mechanical diagrams and (B) equivalent electrical circuit of the hybrid receiver.

The system's response is described by the equation of motion, with x the displacement of the center of mass, and F_{eq} the interaction force between the magnetic field and the receiver magnet:

$$M\ddot{x} = F_{eq} - (K + K_{PE} + K_{ED})x - (D + D_{PE} + D_{ED})\dot{x} \quad (3)$$

We define the mechanical resonance angular frequency ω_0 and the mechanical quality factor Q of the system by:

$$\omega_0 = \sqrt{\frac{K}{M}} \quad (4) \qquad Q = \frac{\sqrt{KM}}{\mathrm{D}} \quad (5)$$

The maximum harvestable power P_0 is defined as the maximum power that a lossless transducer can recover from the mechanical system when no amplitude limit is set. In this case, electrical damping is equal to mechanical damping, and the system is excited at its resonance frequency. This result is analogous to the maximum power recoverable in vibration energy recovery [21].

$$P_0 = \frac{F_{eq}^2 Q}{8M\omega_0} \quad (6)$$

The electrical damping required to fix the displacement at $X = X_l$ with a transducer at the resonance frequency is:

$$D_e(X_l) = \frac{F_{eq}}{\omega_0\, X_l} - D \quad (7)$$

Note that if X_l is chosen to be larger than the amplitude without electrical damping, D_e is negative and does not correspond to an attainable value.

The maximum extracted power associated with this amplitude limit is:

$$P(X_l) = \frac{\omega_0^2\, D_e(X_l)\, X_l^2}{2} \quad (8)$$

This power can be used to predimension the mechanical part of the system.

3.2 Piezoelectric transducer (PE)

The equations of piezoelectricity give the relationship between the piezoelectric output voltage u_{PE} and the displacement x [22]. α_{PE} and C_p are the piezoelectric coefficient and the intrinsic capacitance respectively and $R_{l,PE}$ is the resistive load connected to its terminals. The dielectric losses in the piezoelectric patches are neglected because they are very low compared to the mechanical losses.

$$\begin{cases} F_{eq} - Kx - D\dot{x} - \alpha_{PE}\, u_{PE} = M\,\ddot{x} & (9) \\ \alpha_{PE}\,\dot{x} = \dfrac{u_{\mathrm{PE}}}{R_{l,PE}} + C_p\,\dot{u}_{PE} & (10) \end{cases}$$

From equations 9 and 10, it is possible to express the electrical damping and the electrical stiffness as a function of the operating pulsation of the transmitter ω_e and the load $R_{l,PE}$:

$$\frac{D_{PE}}{D} = \frac{R_{l,PE}\alpha_{PE}^2}{\left(1 + R_{l,PE}^2\omega_e^2 C_p^2\right)D} \quad (11)$$

$$K_{PE} = \frac{R_{l,PE}^2\alpha_{PE}^2 C_p\omega_e^2}{1 + R_{l,PE}^2\omega_e^2 C_p^2} \quad (12)$$

We define the PE coupling Γ_{PE} as the maximum normalized electrical damping.

$$\Gamma_{PE} = \max\left(\frac{D_{PE}}{D}\right) = \frac{\alpha_{PE}^2 Q}{2KC_p} \quad (13)$$

This definition is not the classical state-of-the-art definition of piezoelectric coupling but facilitates comparison with the coupling of the electrodynamic transducer.

The electrical stiffness induced by the PE transduction can change the resonance pulsation ω_r. The limit of variation of the resonance frequency range depends on the PE coupling:

$$\omega_r(R_{l,PE}) \in \left[\omega_0, \omega_0\sqrt{1 + 4\frac{\Gamma_{PE}}{Q^2}}\right] \quad (14)$$

Since the dielectric losses from the PE transducer are neglected, it can extract the maximum recoverable energy P_0 when $\Gamma_{PE} > 1$.

$$\max\left(\frac{P_{PE}}{P_0}\right) = 1 \text{ if } \Gamma_{PE} > 1 \quad (15)$$

In the current state of the art, piezoelectric couplings for cantilever structures span usually between 0.75 and 4, with a maximum equal to 16 [23]. Beyond a coupling of 1, the increase in coupling does not increase maximum power, but it does allow to electrically tune the resonance frequency of the system, especially for wideband vibration energy harvesting. However, such highly coupled prototypes are generally more expensive and more fragile [24].

3.3 Electrodynamic transducer (ED)

The stiffness and energy extracted by the ED transducer from the mechanical system depend on the current flowing through the receiver coil i_{ED} and thus on the electrical load at the transducer output $R_{l,ED}$ [22]:

$$\begin{cases} F_{eq} - K\,x - D\,\dot{x} - \beta_{ED}\,i_{ED} = M\,\ddot{x} & (16) \\ \beta_{ED}\,\dot{x} = \left(R_{l,ED} + R_c\right)\,i_{ED} & (17) \end{cases}$$

β_{ED} and R_c are the ED coefficients and series resistance of the receiver coil, respectively. The effect of the receiver coil inductance is not significant at low frequency (< 1 kHz) and has been neglected. The damping and stiffness induced by the electromagnetic transducer can therefore be expressed by:

$$K_{ED} = 0 \quad (18) \qquad D_{ED} = \frac{\beta_{ED}^2}{R_{l,ED} + R_c} \quad (19)$$

The ED transducer coupling is defined by the normalized maximum electrical damping:

$$\Gamma_{ED} = \max\left(\frac{D_{ED}}{D}\right) = \frac{\beta_{ED}^2}{D\mathrm{R_c}} \quad (20)$$

The power extracted from the ED transducer can also be expressed as:

$$P_{ED}(\omega_e, D_{ED}) = D_{ED}\,\frac{\dot{x}^2(\omega_e, D_{ED})}{2} \quad (21)$$

Contrary to the PE transducer, all the mechanical power extracted is not converted into electrical energy due to the electrical losses. The maximum harvestable power from the ED transducer can then be determined [25]:

$$\max(P_{ED}) = \frac{\Gamma_{ED}}{\Gamma_{ED} + 1}P_0 \quad (22)$$

Γ_{ED} couplings are usually greater than 5, with a maximum being reported of 32 on an energy harvesting device [26]. Very few prototypes with optimized Γ_{ED} were proposed, whether because it often leads to a significant increase of the overall volume and because the maximum output power quickly approaches the maximum recoverable power as the coupling increases ($\max(P_{ED}) > 0.83\,P_0$ for $\Gamma_{ED} > 5$). However, strong electrodynamic couplings allow to efficiently damp the mechanical systems, and thus can limit the mechanical amplitude of the beam.

4 Receiver parameters identification

In the following, the complete model of our system is considered: the mechanical part and the two transducers can be combined using the equations (3), (10) and (17).

$$\begin{cases} F_{eq} - Kx - D\dot{x} - \alpha_{PE}\,u_{PE} - \beta_{ED}i_{ED} = M\,\ddot{x} \\ \alpha_{PE}\,\dot{x} = \dfrac{u_{\mathrm{PE}}}{R_{l,PE}} + C_p\,\dot{u}_{PE} \\ \beta_{ED}\,\dot{x} = \left(R_{l,ED} + R_c\right)\,i_{ED} \end{cases} \quad (23)$$

4.1 Admittance measurement and analysis

To compare our experimental results with the theoretical model, it is necessary to identify the different mechanical and electrical parameters of the proposed prototype. The mechanical damping D is estimated from the amplitude of the system measured with the laser vibrometer when the piezoelectric patch is shorted and the ED transducer is in open circuit. The equivalent mass is obtained by directly measuring the mass of the magnets. To estimate the piezoelectric and electrodynamic couplings Γ_{PE} and Γ_{ED}, the admittances of the two transducers are measured separately for different input voltage amplitudes (i.e. 0.1 V to 2 V for ED only system, and 0.1 V to 10 V for PE only system) over the operating frequency range of the receiver (i.e. 38 Hz to 60 Hz). To perform the admittance measurements, a similar bench configuration as the one mentioned above was used but a sinusoidal voltage is directly applied to the ED or PE transducers via an amplifier. The current i_{ED} or i_{PE} is

measured using a Tektronix TCPA A300 probe, and the amplitude of motion is measured with the laser vibrometer.

The admittance of the PE transducer Y_{PE} is deduced from equations 9 and 10:

$$\underline{Y_{PE}} = \frac{\underline{i_{PE}}}{\underline{u_{PE}}} = \frac{j\omega_e \alpha_{PE}^2}{M\omega_e^2 - K - j\omega_e D} - j\omega_e C_p \qquad (24)$$

For a given rms voltage u_{PE}, the admittance measurements are fitted to determine K, α_{PE} and C_p.

Likewise, the admittance of the ED transducer Y_{ED} is deduced from equations (16) and (17):

$$\underline{Y_{ED}} = \frac{\underline{i_{ED}}}{\underline{u_{ED}}} = \left(\frac{j\omega_e \beta_{ED}^2}{-M\omega_e^2 + K + j\omega_e D} + R_c \right)^{-1} \qquad (25)$$

The admittance measurements are then fitted for a given voltage u_{ED} to determine β_{ED} and R_c. The data are analyzed for a given input voltage as the parameters can vary with the amplitude of motion. Figure 8 shows an example of the impedance analysis of the PE and the ED transducers of the device for $u_{PE} = 1.5\,V$ and $u_{ED} = 0.52\,V$ respectively, given $K = 3865\,N.m^{-1}$, $D = 238\,mN.s.m^{-1}$, $\beta_{ED} = 13.1\,N.A^{-1}$, $R_c = 121\,\Omega$, $\alpha_{PE} = 9.8\,mN.V^{-1}$ and $C_p = 405\,\mu F$ for $M = 35.3\,g$.

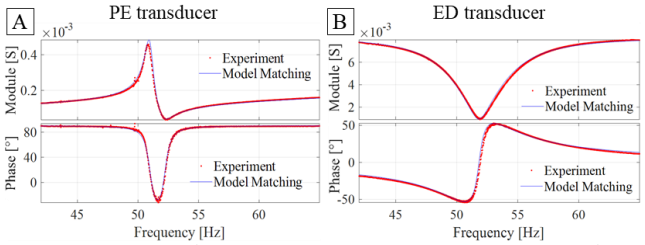

Figure 8: Examples of an admittance analysis and model matching of the (A) PE transducer and (B) the ED transducer.

4.2 *Parameters variation with the motion amplitude*

The model used is linear. As the system studied is not perfectly linear, the measurements show a variation of the parameters with the mass motion amplitude. Figure 9A shows the amplitude of motion of the beam during a frequency sweep for different field amplitudes. One can notice a slight softening effect on the system's response, as the resonance frequency shifts from 49.8 to 45.4 Hz as the mass displacement increases.

Up to 1 mm of peak amplitude of the center of the magnets, the stiffness K decreases by 10 % and the mechanical damping D increases by 45 %. Experimentally, the quality factor decreases with the amplitude of the system (Figure 9B), consequently decreasing the transducers couplings (equations 4 and 5) (Figure 9CD). Furthermore, the admittance analysis indicates no variation of α_{PE}, β_{ED}, R_c and C_p.

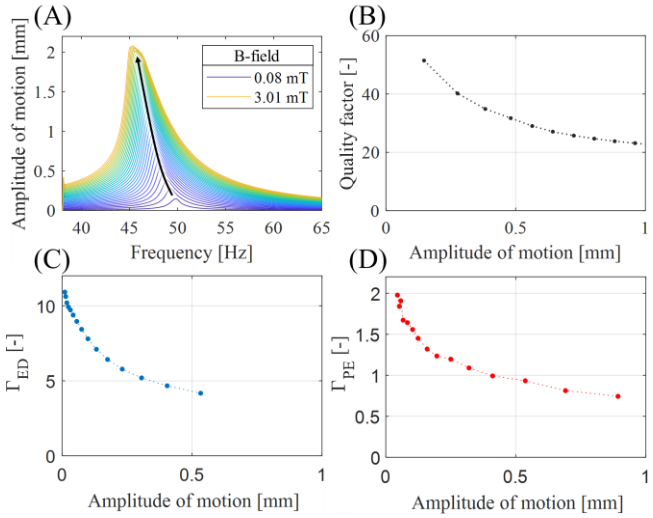

Figure 9: (A) Tip mass's motion amplitude (measurements) as a function of the frequency for different input magnetic fields. (B) Identified quality factor, (C) couplings Γ_{ED} and (D) Γ_{PE} as a function of the motion amplitude.

In the rest of the paper, the identified values reported in Table 1 for an amplitude of 0.7 mm are used as input for the theoretical model. Consequently, a constant mechanical quality factor $Q = 26$ is used, which is a suitable assumption for amplitudes close to 0.7mm.

Table 1: Mechanical and electrical parameters of the receiver at 0.7mm.

Mechanical	PE transducer	ED transducer
$K = 3350\,N.m^{-1}$ $M = 35.5\,g$ $Q = 26$	$C_p = 402\,nF$ $\Gamma_{PE} = 0.88$	$R_c = 121\,\Omega$ $\Gamma_{ED} = 4.1$

4.3 *Comparison between the model and the measurements*

Figure 10 shows the total electrical power of the two transducers (top) and the motion amplitude of the center of the magnet (bottom) as a function of the resistive loads independently connected to the PE and ED transducers for an input field amplitude B_0 of 1.38 mT peak. The results of the theoretical model were carried out with the parameter set from Table 1 at the resonance.

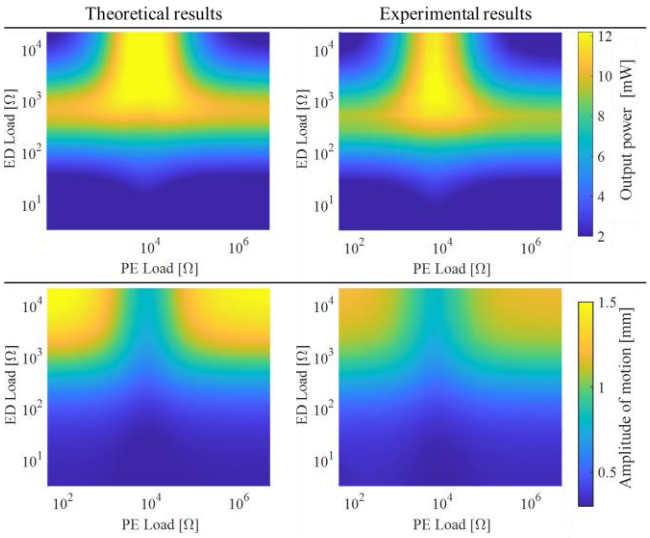

Figure 10: Comparison between measurements and the model for the power and amplitude of motion at the resonance frequency as a function of the resistive loads applied to the transducers, for B_0 of 1.38 mT peak.

One can note that there is a good agreement between the experimental and theoretical results, both for the amplitude of motion and the power output. As the amplitude of motion increases away from 1 mm, the deviation between the model and the theoretical results increases due to the variation of the quality factor with the amplitude, which is particularly the case for large field amplitudes or for low electrical damping. The amplitude of motion error is less than 2% for different simulations and measurements at 0.7 mm amplitude, and 10% for 1 mm amplitude. For output power, the error is around 4% for an amplitude of around 0.7 mm, and between 10 and 30 % for an amplitude of 1 mm.

5 Power output vs magnetic field amplitude

5.1 *Limitation of the amplitude of motion*

The mechanical stresses in the structure are directly related to the amplitude of motion, and large stresses lead to premature aging of the system or to breakage. To protect the system, we aim at limiting the range of motion by an electrically-induced damping. In the following, this limit is set at $X_l = 0.7$ mm. The linearized model presented previously is therefore adapted to this range. The output power and voltage amplitudes of the transducers are evaluated as a function of the amplitude of the magnetic field (0.15 to 4.5 mT) for different electrical loads (44.5 Ω to 5 MΩ for the PE transducer, 3 Ω to 20 MΩ for the ED transducer). For each mapping, the maximum harvested power with an amplitude lower than 0.7 mm is recorded.

Three cases are compared: the ED transducer alone, the PE transducer alone, and the hybrid system with both transducers.

- **PE only:** The PE transducer alone converts mechanical energy into electrical energy, the ED transducer being in open circuit (D_{ED}= 0).
- **ED only:** The ED transducer alone converts mechanical energy into electrical energy, the PE transducer being in short circuit (D_{PE}= 0, K_{PE}=0).
- **Hybrid:** Both transducers are used simultaneously with their respective resistive loads. The optimal loads that give the highest output power are reported.

Output powers for the optimal loads for $X_l \leq 0.7\ mm$ as a function of the magnetic field are reported in Figure 11. The theoretical maximum power P_0 with no amplitude limitation is given by the black dashed line.

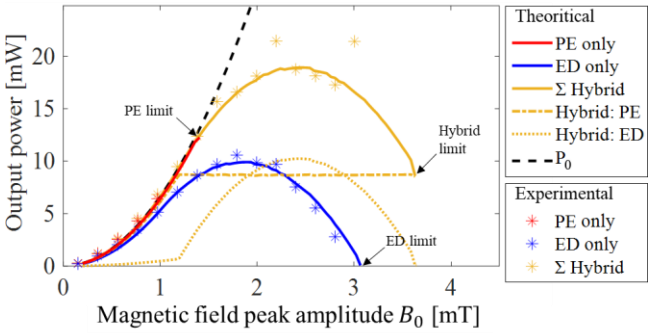

Figure 11: Electrical power output versus magnetic field peak amplitude for a maximum range of motion of 0.7 mm.

In the case of weak magnetic fields generated by the transmitter coil (up to 1.2 mT), the amplitude of motion is lower than $X_l = 0.7\ mm$ and no electrical overdamping is required. On the PE-only system, the PE transducer has a high enough coupling, allowing the maximum electrical damping to be close to the optimum damping. Moreover, as the dielectric losses are low, the power obtained over this range of magnetic fields is close to the maximum reachable power P_0. On the other hand, ED-only system has a high enough electrical damping to extract the maximum mechanical power. The difference between the output power and the maximum obtainable power P_0 is due to the resistive losses in the coil. On the hybrid system, the maximum harvested power (sum of the PE and ED transducer's electrical powers) is the same as the PE-only configuration. Consequently, the ED transducer is not useful for weak magnetic fields conditions.

For input magnetic fields greater than 1.2 mT, it is necessary to increase the electrical damping of the transducers to limit the amplitude of motion to $X_l = 0.7$ mm. The PE-only configuration is not able to damp the system enough to limit its amplitude since its maximum damping is close to the optimal damping ($D_{PEmax} \approx D$). Therefore, the PE alone cannot operate above 1.2 mT without exceeding the displacement limit. As for the ED only configuration, it can overdamp the system enough to limit the motion amplitude at the expense of the harvested power. In this displacement range, the optimal load decreases until it reaches zero to keep the amplitude at 0.7 mm. Therefore, the output voltage decreases as the magnetic field increases. In this case, the maximum allowable magnetic field without exceeding the motion amplitude of 0.7 mm is around 3 mT. Concerning the hybrid system, since the PE coupling is about 1 and is considered lossless, the PE operates at optimum load to harvest the maximum mechanical energy. Meanwhile, the ED transducer load decreases to zero in order to limit the motion amplitude. When the maximum damping of the ED transducer is reached, the system is no longer able to limit its amplitude. This limit is reached at higher magnetic field amplitudes than the other configurations thanks to the addition of ED and PE electric damping, while recovering

higher power due to the PE transducer operating at optimum load over the entire range. Indeed, the maximum allowable magnetic field for the hybrid system is 3.6 mT, compared to 1.4 mT and 3.1 mT respectively for the PE only and ED only systems. Moreover, the hybrid system allows to increase the harvested power by 84 % (at 2 mT) compared to the ED-only configuration.

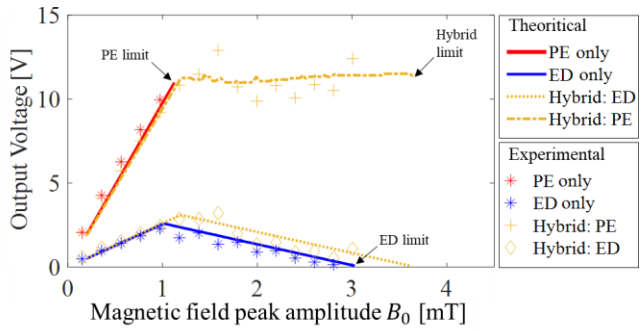

Figure 12: Electrical voltage versus magnetic field peak amplitude for a maximum range of motion of 0.7 mm.

The ED and PE rms voltage values are plotted as a function of B_0 in Figure 12. In the case of the hybrid configuration, both the ED and PE voltages are shown. The ED transducer voltage is low in the following cases:

- For low input amplitudes when the motion amplitude of the mass is low.
- For high amplitudes when it is necessary to limit the motion amplitude by decreasing the output load.

5.2 *Impact of couplings on output power at fixed amplitude*

Changing the geometry or the materials of the receiver affect the couplings of the two transducers [27], [28]. With the analytical model developed in section 3, the maximum recoverable power at fixed amplitude and magnetic field can be obtained as described in equation (8). Figure 13 shows the normalized maximum recoverable power with an amplitude limitation of $X_l = 0.7\ mm$ and for $B_0 = 1.5\ mT$ (Figure 13 A) and for $B_0 = 3.5\ mT$ (Figure 13 B) while varying the couplings by changing the coefficients α_{PE} and β_{ED}.

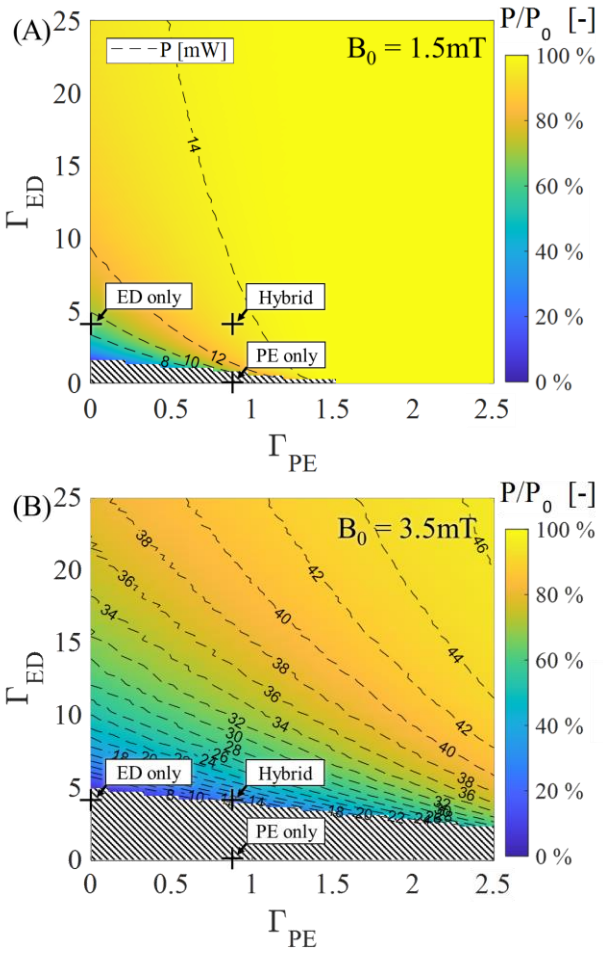

Figure 13: Harvested electrical power (isovalue lines) and normalized power of the maximum recoverable power (map) at the optimal loads as a function of Γ_{ED} and Γ_{PE} couplings for (A) 1.5 mT and (B) 3.5 mT The hatched area represents the area in which it is impossible to limit the amplitude below 0.7 mm.

For a 1.5 mT field (Figure 13A), for weak PE and ED coupling, the total electrical damping is not sufficient to limit the amplitude below 0.7 mm. PE-only systems do not work for couplings less than 1.5 and recover 100 % of the maximum energy beyond this value. The ED-only systems allow to obtain 60 % of the maximum recoverable energy from a coupling of 4 and 80 % from a coupling of 10. The hybrid prototype made in this work provides almost 100 % of the energy despite the limited piezoelectric coupling and the electrical losses of the ED transducer.

At higher field intensity of 3.5 mT (Figure 13B), PE-only systems cannot limit the motion to 0.7 mm. For ED-only systems, a coupling of 5 is necessary to limit the amplitude. In the case of our system, this coupling is only reached when both transducers are active. However, stronger couplings are necessary to recover the maximum power (maximum power 5.4 times higher for 3.5 mT than for 1.5 mT).

6 Discussion

The receiver studied in this paper is a vibrating system. Wireless power transmission systems are frequently mentioned as an alternative to power cables in mobile applications. Such systems can be made to be moved freely in space. However, due to the large variation of the magnetic

field generated by the transmitter, the receiver might be subjected to high field, and the amplitude of motion of the center of mass might increase dramatically. The robustness of these systems is closely related to their range of motion It is then necessary to limit the amplitude of motion of these structures when the magnetic field is too strong to guarantee a long lifespan.

In addition, when designing a WPT system, the range of magnetic field that the receiver will experience over the space should be assessed. If the system is too weakly coupled, the electrical damping does not allow a large range of admissible magnetic field: the system will have to be operated at optimum load or be oversized. As shown in this paper, increasing the electromechanical coupling increases the range of admissible magnetic field without oversizing the receiver.

Nevertheless, when designing a EWPT system, the three configurations (PE alone, ED alone or hybrid configuration) must be considered. The efficiency, cost, volume, and robustness of each solution varies, making the choice very dependent on the environment of the sensor node.

The first possible solution is a receiver based on PE transduction as strongly coupled as possible. This method allows the structure to be overdamped while maintaining an interesting power density. In addition, this system is beneficial in terms of output voltages in order to be compatible with the voltages requirements of the WSN power management circuit. The drawback of such a system is the cost of the strongly coupled PE materials. A typical situation that may lead to the choice of the PE-only configuration is when the receiver will be exposed to a small variation in magnetic fields.

A second solution is the implementation of a receiver based on ED transduction only. This transducer can strongly overdamp the mechanical structure with no contact. Its main drawback is the volume used by the receiver coils to achieve a reasonably large coupling. Indeed, a large coupling requires a large amount of copper and consequently results in a large increase in the size and volume of the device. In addition, the voltages at the terminals of the receiver coils are lower and not easily exploitable by the WSN, unless small wires are used, which can pose problems, particularly in the case of miniaturized systems. In the situation where long lifetimes are required and the input magnetic fields are high, the use of a purely electrodynamic receiver is probably the best solution.

Finally, the last configuration is a receiver based on a hybrid transduction as proposed in this work. This method has the advantage of obtaining a large coupling from two loosely coupled transducers. The operating magnetic field range is larger, with higher output voltages thanks to the PE transducer at low magnetic fields, and high damping at high fields thanks the ED transducer. On the other hand, this system requires a more complex power management circuit with two electrical outputs. When the system is to be subjected to a large variation in input magnetic field during its lifespan, or when the system has to be miniaturized, the use of a hybrid system is a solution to be considered.

7 Conclusion

This paper presents the electrical damping capabilities of electrodynamic wireless power transmission systems with piezoelectric and electrodynamic transducers or both (hybrid systems), with the aim of limiting the wear and tear of the system during overstress.

A hybrid experimental receiver was used for this purpose, consisting of a cantilever beam with a magnet placed at its free end. Piezoelectric layers are embedded in the vibrating beam and two receiver coils are placed near the magnet to convert the energy. The electrodynamic transducer exhibits a strong coupling allowing a strong electrically induced damping to protect the structure in case of high input field. The PE transducer has a weaker coupling but is lossless and can provide higher voltages that can be more easily exploited by AC-DC converters. The dual electromechanical transduction allows to significantly limit the vibration amplitude to prevent premature aging of the receiver when subjected to high magnetic field amplitude. To demonstrate this feature, a maximum tip mass amplitude was set to protect the receiver while harvesting the maximum power. The amplitude limitation is achieved by the electrical damping of the transducers. In the case where the amplitude is limited to 0.7 mm, 19 mW can be recovered at 2.5 mT. The system can withstand 3.6 mT without exceeding the amplitude limit which is significantly higher than when using only the PE-only or ED-only configurations. Further research will focus on reducing and optimizing the size of the prototype, and on implementing power management circuits based on extraction techniques dedicated to EWPT hybrid systems with the aim of limiting the wear and tear of the system during overstress to increase its robusteness.

8 Acknowledgements

This work was conducted as part of the strategic scientific collaboration between SYMME, Université Savoie Mont-Blanc and the French Alternative Energies and Atomic Energy Commission.

9 References

[1] H. Elahi, K. Munir, M. Eugeni, S. Atek, and P. Gaudenzi, ‘Energy harvesting towards self-powered iot devices’, *Energies*, vol. 13, no. 21, 2020, doi: 10.3390/en13215528.

[2] Md. A. Ullah, R. Keshavarz, M. Abolhasan, J. Lipman, K. P. Esselle, and N. Shariati, ‘A Review on Antenna Technologies for Ambient RF Energy Harvesting and Wireless Power Transfer: Designs, Challenges and Applications’, *IEEE Access*, vol. 10, pp. 17231–17267, 2022, doi: 10.1109/ACCESS.2022.3149276.

[3] M. Z. Erel, K. C. Bayindir, M. T. Aydemir, S. K. Chaudhary, and J. M. Guerrero, ‘A Comprehensive Review on Wireless Capacitive Power Transfer Technology: Fundamentals and Applications’, *IEEE Access*, vol. 10, pp. 3116–3143, 2022, doi: 10.1109/ACCESS.2021.3139761.

[4] O. Freychet *et al.*, 'A Versatile Through-Metal-Wall Acoustic Power and Data Transfer Solution', in *2019 19th International Conference on Micro and Nanotechnology for Power Generation and Energy Conversion Applications (PowerMEMS)*, Dec. 2019, pp. 1–6. doi: 10.1109/PowerMEMS49317.2019.92321100357.

[5] N. Garraud, D. Alabi, S. Chyczewski, J. D. Varela, D. P. Arnold, and A. Garraud, 'Extending the range of wireless power transmission for bio-implants and wearables', *J. Phys.: Conf. Ser.*, vol. 1052, p. 012023, Jul. 2018, doi: 10.1088/1742-6596/1052/1/012023.

[6] N. Garraud, A. Garraud, D. Munzer, M. Althar, and D. P. Arnold, 'Modeling and experimental analysis of rotating magnet receivers for electrodynamic wireless power transmission', *J. Phys. D: Appl. Phys.*, vol. 52, no. 18, p. 185501, Feb. 2019, doi: 10.1088/1361-6463/ab0643.

[7] W. Li, 'High efficiency wireless power transmission at low frequency using permanent magnet coupling', University of British Columbia, 2009. doi: 10.14288/1.0067661.

[8] A. Ameye *et al.*, 'Enabling IOT Wireless Distant Charging: 7.9-Mw Integrated Power Receiver at 30 cm', in *2022 21st International Conference on Micro and Nanotechnology for Power Generation and Energy Conversion Applications (PowerMEMS)*, IEEE, 2022, pp. 311–312.

[9] B. D. Truong, D. Wang, T. Xue, S. Trolier-Mckinstry, and S. Roundy, 'Experiments on a wireless power transfer system for wearable device with sol-gel thin-film PZT', presented at the Journal of Physics: Conference Series, 2019. doi: 10.1088/1742-6596/1407/1/012063.

[10] B. D. Truong and S. Roundy, 'Wireless power transfer system with center-clamped magneto-mechano-electric (MME) receiver: model validation and efficiency investigation', *Smart Mater. Struct.*, vol. 28, no. 1, p. 015004, Nov. 2018, doi: 10.1088/1361-665X/aaeb6a.

[11] Y. Chen, Y. Cheng, Y. Jie, X. Cao, N. Wang, and Z. L. Wang, 'Energy harvesting and wireless power transmission by a hybridized electromagnetic–triboelectric nanogenerator', *Energy Environ. Sci.*, vol. 12, no. 9, pp. 2678–2684, 2019, doi: 10.1039/C9EE01245A.

[12] M. Renaud *et al.*, 'Optimum power and efficiency of piezoelectric vibration energy harvesters with sinusoidal and random vibrations', *J. Micromech. Microeng.*, vol. 22, no. 10, p. 105030, Sep. 2012, doi: 10.1088/0960-1317/22/10/105030.

[13] Y. Zhang, T. Wang, A. Luo, Y. Hu, X. Li, and F. Wang, 'Micro electrostatic energy harvester with both broad bandwidth and high normalized power density', *Applied Energy*, vol. 212, pp. 362–371, Feb. 2018, doi: 10.1016/j.apenergy.2017.12.053.

[14] I. Jung *et al.*, 'Design principles for coupled piezoelectric and electromagnetic hybrid energy harvesters for autonomous sensor systems', *Nano Energy*, vol. 75, p. 104921, Sep. 2020, doi: 10.1016/j.nanoen.2020.104921.

[15] R. M. Toyabur, M. Salauddin, H. Cho, and J. Y. Park, 'A multimodal hybrid energy harvester based on piezoelectric-electromagnetic mechanisms for low-frequency ambient vibrations', *Energy Conversion and Management*, vol. 168, pp. 454–466, Jul. 2018, doi: 10.1016/j.enconman.2018.05.018.

[16] C. Wang, S.-K. Lai, J.-M. Wang, J.-J. Feng, and Y.-Q. Ni, 'An ultra-low-frequency, broadband and multi-stable tri-hybrid energy harvester for enabling the next-generation sustainable power', *Applied Energy*, vol. 291, 2021, doi: 10.1016/j.apenergy.2021.116825.

[17] M. A. Halim, A. A. Rendon-Hernandez, S. E. Smith, and D. P. Arnold, 'Analysis of a Dual-Transduction Receiver for Electrodynamic Wireless Power Transfer', *IEEE Transactions on Power Electronics*, vol. 37, no. 6, pp. 7470–7479, Jun. 2022, doi: 10.1109/TPEL.2022.3140777.

[18] B. D. Truong, C. P. Le, and S. Roundy, 'Piezoelectric–Electromagnetic Hybrid Energy Harvesting System: When is it Useful?', in *2022 21st International Conference on Micro and Nanotechnology for Power Generation and Energy Conversion Applications (PowerMEMS)*, Dec. 2022, pp. 200–203. doi: 10.1109/PowerMEMS56853.2022.10007615.

[19] P. D. Mitcheson, T. C. Green, E. M. Yeatman, and A. S. Holmes, 'Architectures for vibration-driven micropower generators', *Journal of Microelectromechanical Systems*, vol. 13, no. 3, pp. 429–440, Jun. 2004, doi: 10.1109/JMEMS.2004.830151.

[20] E. Halvorsen, C. P. Le, P. D. Mitcheson, and E. M. Yeatman, 'Architecture-independent power bound for vibration energy harvesters', *J. Phys.: Conf. Ser.*, vol. 476, no. 1, p. 012026, Dec. 2013, doi: 10.1088/1742-6596/476/1/012026.

[21] A. Badel and E. Lefeuvre, 'Nonlinear Conditioning Circuits for Piezoelectric Energy Harvesters', in *Nonlinearity in Energy Harvesting Systems*, E. Blokhina, A. El Aroudi, E. Alarcon, and D. Galayko, Eds., Cham: Springer International Publishing, 2016, pp. 321–359. doi: 10.1007/978-3-319-20355-3_10.

[22] E. Arroyo, A. Badel, F. Formosa, Y. Wu, and J. Qiu, 'Comparison of electromagnetic and piezoelectric vibration energy harvesters: Model and experiments', *Sensors and Actuators A: Physical*, vol. 183, pp. 148–156, Aug. 2012, doi: 10.1016/j.sna.2012.04.033.

[23] A. Badel and E. Lefeuvre, 'Wideband Piezoelectric Energy Harvester Tuned Through its Electronic Interface Circuit', *J. Phys.: Conf. Ser.*, vol. 557, no. 1, p. 012115, Nov. 2014, doi: 10.1088/1742-6596/557/1/012115.

[24] Z. Yang and J. Zu, 'Comparison of PZN-PT, PMN-PT single crystals and PZT ceramic for vibration energy harvesting', *Energy Conversion and Management*, vol. 122, pp. 321–329, Aug. 2016, doi: 10.1016/j.enconman.2016.05.085.

[25] V. R. Challa, S. Cheng, and D. P. Arnold, 'The role of coupling strength in the performance of electrodynamic vibrational energy harvesters', *Smart Mater. Struct.*, vol. 22, no. 2, p. 025005, Dec. 2012, doi: 10.1088/0964-1726/22/2/025005.

[26] V. Ordoñez, R. Arcos, and J. Romeu, ‘A high-performance electromagnetic vibration energy harvester based on ring magnets with Halbach configuration’, *Energy Conversion and Management: X*, vol. 16, p. 100280, Dec. 2022, doi: 10.1016/j.ecmx.2022.100280.

[27] D. Gibus, P. Gasnier, A. Morel, S. Boisseau, and A. Badel, ‘Modelling and design of highly coupled piezoelectric energy harvesters for broadband applications’, *J. Phys.: Conf. Ser.*, vol. 1407, p. 012009, Nov. 2019, doi: 10.1088/1742-6596/1407/1/012009.

[28] G. Delattre, S. Vigne, A. Brenes, N. Garraud, O. Freychet, and S. Boisseau, ‘A new approach to design electromagnetic transducers for wideband electrically-tuned vibration energy harvesting’, *Journal of Intelligent Material Systems and Structures*, vol. 34, no. 11, pp. 1314–1329, Jul. 2023, doi: 10.1177/1045389X221135017.

